Eur. Phys. J. E (2011) **34**: 61
DOI 10.1140/epje/i2011-11061-4

THE EUROPEAN PHYSICAL JOURNAL E

Regular Article

Microstructuration stages during gelation of gelatin under shear

O. Ronsin[a], C. Caroli, and T. Baumberger

Institut des Nanosciences de Paris, CNRS UMR 7588, Université Pierre et Marie Curie, 4 place Jussieu, 75005 Paris, France

Received 25 January 2011 and Received in final form 22 March 2011
Published online: 24 June 2011 –

Abstract. We study gelation under shear of aqueous gelatin by measuring the evolution of the apparent viscosity, thus extending the previous study by de Carvalho and Djabourov (W. de Carvalho, M. Djabourov, Rheol. Acta **36**, 591 (1997)). From a set of experiments under constant stress, we deduce that the microstructure evolves through the following succession of regimes: i) nucleation and growth until crowding of a microgel suspension; ii) coalescence into strata parallel to the flow; iii) gradual thickening of these strata via transverse cross-linking until the flow finally localizes into two interfacial sliding bands which close sequentially. The transition between these regimes occurs at characteristic *viscosity* values. This scenario is fully confirmed by experiments performed at constant shear rates. We expect it to be relevant for all materials forming thermoreversible gels.

1 Introduction

Gelation under shear has repeatedly been proposed as a method for tailoring microstructured fluids or pastes [1–5]. However, the relation between the shear history during gelation and the final gel rheological properties is still far from being fully unraveled. Studies in this field were pioneered by de Carvalho and Djabourov [6] who have characterized in detail, along the course of the gelation process, the dynamic evolution of the rheological response of gelatin —a widely studied self-assembling biopolymer which forms thermoreversible hydrogels cross-linked by triple-helix segments reminiscent of the native collagen structure [7]. They interpreted their results in terms of the formation of a suspension of microgel particles whose size grows up to a $\dot{\gamma}$-dependent limit. They concluded to the existence of a threshold shear rate $\dot{\gamma}^\star$ below which this limiting value would be large enough for percolation to occur and result in the formation of a weak particulate gel.

Later studies have concentrated on comparing systems once they have been formed under either quiescent or flowing conditions. In particular, Norton and coworkers [2,3] have proved the feasibility of controlled "fluid gels" (stable suspensions of microgel particles). They obtained them via gelation under shear of solutions of biopolymers (agar [2], κ-carrageenan [3]) undergoing spinodal decomposition. Altmann *et al.* [1] and Caggioni *et al.* [5] have shown that applying shear during gelation may result in substantial modifications of the mechanical response. From this, they infer that, even when shearing does not impede full gelation, it certainly affects the gel microstructure.

[a] e-mail: olivier.ronsin@insp.jussieu.fr

These results suggest the following remark: a gelling solution close to percolation can be viewed as a concentrated suspension of microgel clusters (the size distribution of which depends on the shearing rate, if any). On the other hand, a number of works have shown, in the last two decades, that concentrated suspensions frequently exhibit shear banding [8]. The question then naturally arises of whether flow localization could be relevant to gelation under shear —an issue of importance in terms of microstructure formation. Indeed, if so, the resulting gels could be expected to exhibit specific anisotropies, possibly dependent upon the flow history.

With this question in mind, we revisit here the gelation dynamics of sheared gelatin, paying special attention to the dense microgel regime, which was overlooked in ref. [6]. We extend the results of de Carvalho and Djabourov by closely analyzing, in experiments performed under constant stress σ (sect. 3), the later stages of the dynamics, as characterized by the evolution of the apparent viscosity $\eta_\sigma(t)$, which increases by about six orders of magnitude up to full gelation of the system. We find that the $\log \eta_\sigma$ *vs.* t curves (see fig. 2) exhibit a three-step structure, whose breaks of slope occur at values of η_σ independent of the imposed shear stress, which strongly suggests that they signal transitions between well-defined microstructural regimes.

This leads us to propose that, after initial nucleation and growth of a homogeneous microgel system (stage I), gelling proceeds via coalescence into strata parallel to the flow (stage II), which gradually thicken via transverse cross-linking while the flow becomes increasingly localized (stage III), until gel percolation is complete, but for two sliding bands along the rheometer plates. The final

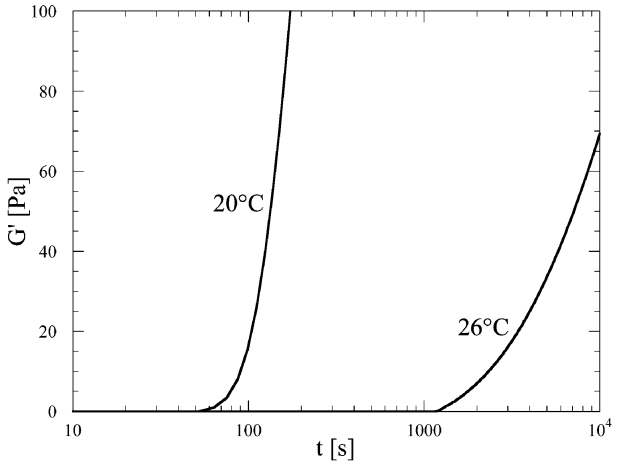

Fig. 1. Storage modulus G', measured at 1 Hz and strain amplitude 10^{-3}, *versus* time t after quench at $T = 20$ and 26 °C, for a 5 wt% gelatin solution in water.

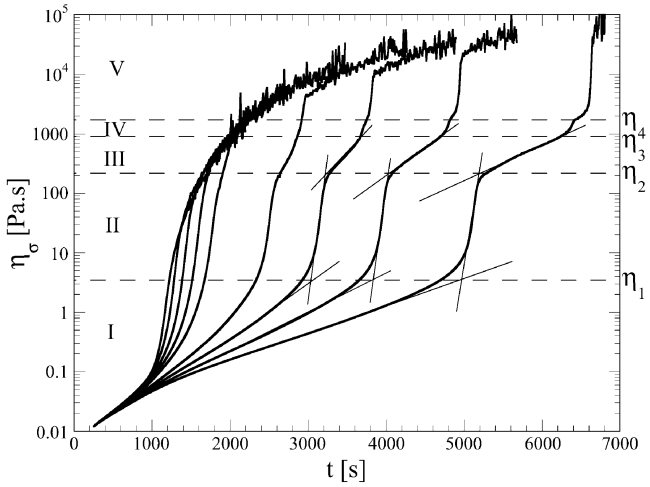

Fig. 2. Apparent viscosity $\eta_\sigma = \sigma/\dot{\gamma}$ measured during gelation of a 5 wt% sample under imposed stress *versus* time t after quenching at $T = 26$ °C. From left to right $\sigma = 1$, 2, 3, 4, 5, 8, 10, 12, 15 Pa. The characteristic viscosities $\eta_1 \ldots \eta_4$ label the limits separating regimes I to IV (see text).

evolution towards full gelation consists of the sequential closure of these two bands.

We then show (sect. 4) that this qualitative scenario is fully consistent with the time evolution of $\eta_{\dot{\gamma}}(t)$, measured in experiments performed over a wide range of imposed shear rates. This suggests, in particular, that gels formed under moderate or low shear rates should present a layered texture resulting in an anisotropic fracture energy (toughness).

2 Experimental

2.1 Sample preparation

When cooled below $T_{\rm gel} \simeq 29$ °C, aqueous gelatin solutions form thermoreversible gels, whose mechanical properties depend on their thermal history. Under quiescent conditions, following a rapid quench down to $T < T_{\rm gel}$, after a latency time τ, the low-frequency ($\nu = 0.1$–100 Hz) storage modulus G' builds up rapidly, then reaches a logarithmic, apparently unbounded, growth regime [7] associated with the slow growth and rearrangements of the cross-linking segments. As illustrated in fig. 1, the lower T is, the faster the kinetics —*i.e.* the smaller τ and the larger the log-slope of the storage modulus.

We prepare 5 wt% solutions of gelatin (Sigma, type A from porcine skin, 300 Bloom) stirred at 65 °C in deionized water. The pre-gel solution is then poured into the cone-plate cell (diameter 50 mm, angle 2°, sandblasted) of a stress-controlled rheometer (Anton Paar, MCR 501) thermalized to within 0.1 °C. The sample is protected against water evaporation by a dodecane rim.

A reference state of the sol is obtained by pre-shearing at $T = 45$ °C, $\dot{\gamma} = 1\,{\rm s}^{-1}$ for 200 s. For $\dot{\gamma} < 100\,{\rm s}^{-1}$, we measure its viscosity to be $3 \cdot 10^{-3}$ Pa s. We then establish the prescribed stress, or strain rate, and subsequently quench to the working temperature $T = 26$ °C. This temperature is chosen close below $T_{\rm gel}$, so that the gelling kinetics (see fig. 1) be slow enough for the quenching time (80 s) to be negligible. That is, the whole gelation process occurs under isothermal conditions.

After each run, the cell is cleaned and a new sample is prepared from the same pre-gel stock solution. We have checked that this protocol ensures reproducibility of the characteristic viscosities (see sect. 3) on the $\eta_\sigma(t)$ curves to within 10%.

2.2 Shearing protocol

Experiments under controlled strain rate are performed for $\dot{\gamma}$ ranging from 10^{-2} to $10^2\,{\rm s}^{-1}$, shear being applied at its prescribed value prior to quenching.

We perform stress-controlled experiments for values of σ ranging from 0.5 to 15 Pa. Under the initial shear rate of $5000\,{\rm s}^{-1}$ corresponding to $\sigma = 15$ Pa, the sol is found to be expelled out of the cell. This leads us to adopt the following protocol. Before quenching, we apply a low stress $\sigma_0 = 1$ Pa (initial $\dot{\gamma}$ of $300\,{\rm s}^{-1}$) which protects the system against centrifugation, then quench and wait under σ_0 for a time $t_0 = 250$ s after quench before switching to the prescribed higher stress level. The duration of the associated stress transient [9] is ~ 30 s. We have checked that the further evolution of η is insensitive to i) reductions of t_0 within the range accessible at each σ-level and ii) the value of the pre-shear stress σ_0 in the range from 0.5 to 2 Pa.

3 Gelation under constant stress

Figure 2 shows the time evolution of the apparent viscosity $\eta_\sigma = \sigma/\dot{\gamma}$ measured during gelation under various stress levels, ranging from 1 to 15 Pa. Clearly, increasing

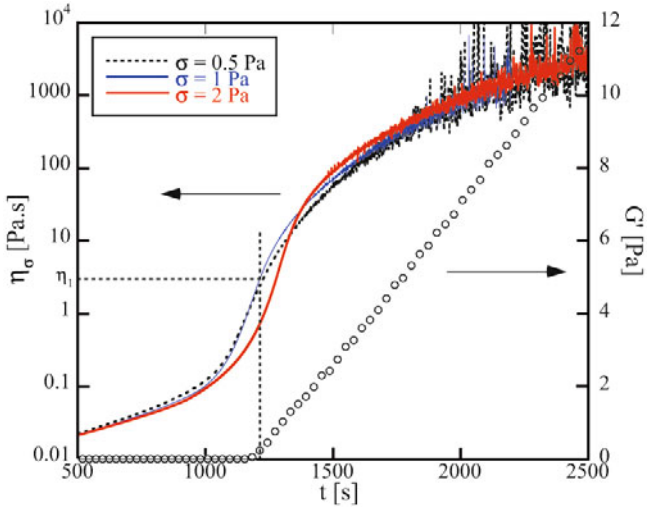

Fig. 3. Viscosity η_σ measured during gelation under low stress levels $\sigma = 0.5, 1, 2\,\mathrm{Pa}$ *versus* time t after quench. Circles: storage modulus G' (at 1 Hz, strain amplitude 10^{-3}) of the same gelatin solution gelling under quiescent conditions. $\eta_1 \simeq 3\,\mathrm{Pa\,s}$ is the viscosity at the end of regime I (see text).

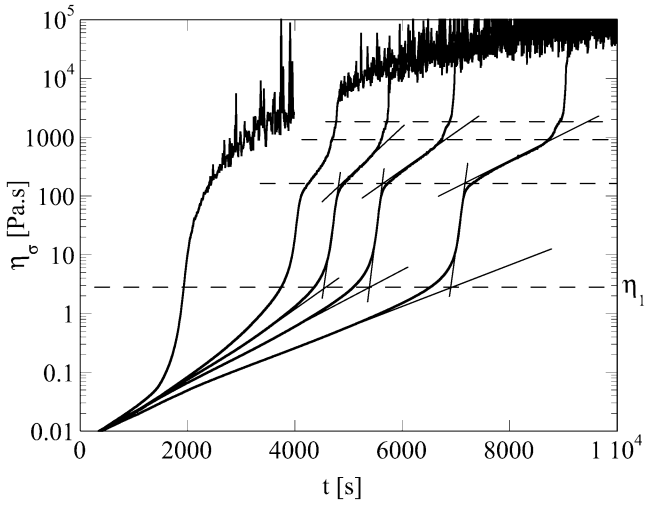

Fig. 4. Apparent viscosity $\eta_\sigma = \sigma/\dot\gamma$ measured during gelation of a 4 wt% sample under imposed stress *versus* time t after quenching at $T = 26\,^\circ\mathrm{C}$. From left to right $\sigma = 1, 5, 6, 7, 8\,\mathrm{Pa}$.

σ results in a substantial slowing down of the gelling kinetics. However, we find that this effect only shows up for $\sigma > 1\,\mathrm{Pa}$, while (see fig. 3) up to this value, the viscosity curves are indistinguishable within experimentally accuracy and can thus be considered as probing gelation under quiescent conditions. In this quasi-quiescent limit $\log \eta_\sigma$ exhibits a sigmoidal shape ending in an ultra-slow regime (noisier part of the curves[1]) where it measures the creep viscosity of bulk gel undergoing the above-mentioned slow aging process [10,11].

As σ increases up to about 5 Pa, the sigmoidal shape (see fig. 2) is essentially preserved while gradually stretching along the time axis. At higher stress levels, a stepped substructure becomes increasingly conspicuous. One is naturally tempted to associate the marked breaks of the slope $\mathrm{d}(\log \eta_\sigma)/\mathrm{d}t$ with structural transitions in the flowing system. This is further supported by the observation (see fig. 2) that, strikingly enough, each of the four slope breaks (i: $1, \ldots, 4$) occurs at a characteristic (quasi σ-independent) viscosity level η_i.

In order to test the robustness of these features, we have performed a similar set of experiments on a 4% gelatin solution. This concentration difference results in a substantial increase, by a factor $\simeq 1.6$, of the quiescent gelation time. As shown in fig. 4, while the dynamics is globally slowed down, all the above-described qualitative features of the viscosity response are preserved.

This leads us to hypothesize the existence of a well-defined sequence of regimes. The earliest stage ($\eta_\sigma < \eta_1$), which we label I, certainly corresponds to the one analyzed in [6], in which cross-links nucleate [12], thereby generating microgel clusters which grow at a rate limited by the flow, but whose volume fraction remains below the crowding threshold, the flow being homogeneous on the mesoscopic scale. This regime terminates when the viscosity of this thickening suspension reaches the threshold value η_1 which we find to be stress-independent. According to [6], termination should occur when the microgel suspension reaches the percolation threshold. If such is actually the case, the time at which η_1 is reached under quasi-quiescent conditions should therefore coincide with the emergence of a finite storage modulus in the non-flowing system. This is very nicely confirmed by the data shown in fig. 3.

Furthermore, it appears (see figs. 2 and 4) that the value of η_1 is the same, $\simeq 3\,\mathrm{Pa\,s}$, for both the 5 and 4 wt% systems at the same temperature $T = 26\,^\circ\mathrm{C}$, although this level is reached at markedly different times for a given applied stress. This observation is consistent with η_1 marking the percolation threshold of rigid particles, which occurs at a fixed microgel packing fraction. This suggests that, at this stage, the shear modulus of the microgels is already much larger than the imposed stresses ($\lesssim 15\,\mathrm{Pa}$).

At low stress levels ($\sigma \lesssim 5\,\mathrm{Pa}$), increasing the applied stress clearly slows down the growth of the microgel suspension. However, crowding does not results in any clearly identifiable feature on the $\eta_\sigma(t)$ curves.

In contradistinction, under applied stresses $\sigma \gtrsim 5\,\mathrm{Pa}$, crowding is followed by a sudden rise of η_σ: most likely, in this regime, the resulting sparse percolating network is too weak to sustain the build-up of elastic stresses in the rotating cell, and the system enters a regime where microgel cross-linking competes with "breaking" by H-bond dissociation under the flow-induced stresses. In our simple shear configuration, clearly, breaking occurs preferentially between layers parallel to the mean flow. We thus expect the system to develop an anisotropic structure of more strongly cross-linked cluster strata sliding viscously on each other.

This second stage (phase II), characterized by a very steep increase of η_σ over about two orders of magnitude, we observe to switch, for $\eta_\sigma = \eta_2 \approx 220\,\mathrm{Pa\,s}$, to a third

[1] The high noise level in this regime originates from the instrumental $\dot\gamma$ resolution, of order $10^{-3}\,\mathrm{s}^{-1}$.

stage (III) with a substantially smaller viscosity growth rate. Most likely, this slope break signals the transition to a regime where elementary strata gradually thicken via permanent (or long-lived intermittent) cross-linking, the flow becoming increasingly localized into a random fracture-like structure akin to that seen in sheared transient network systems [13,14]. As this evolution proceeds, the thickness of cohesive layered blocks increases until the gel fills the whole cell gap, except for a last sliding band, the closure of which corresponds to the abrupt jump of η_σ to its creep value.

However, one observes (see fig. 2) that this final jump is preceded by a much smaller step. Moreover, strikingly enough, the two associated apparent viscosity values verify

$$\frac{\eta_4}{\eta_3} \cong 2. \tag{1}$$

Now, assume that there are, in a cell of thickness e, two flow bands, each of thickness h, with the same rheology $\sigma = f(\dot{\gamma}_{\rm loc})$, where the local and external shear rates are related by $\dot{\gamma} = \dot{\gamma}_{\rm loc}(2h/e)$. When one of them closes at fixed σ, $\dot{\gamma}_{\rm loc}$ is preserved while, now, $\dot{\gamma} = \dot{\gamma}_{\rm loc}(h/e)$, so that the apparent viscosity doubles. Relation (1) thus clearly indicates that, at the end of stage III, the flow has localized into two bands of equal thicknesses, which close sequentially. Their symmetry strongly suggests that these two bands are located along the cell walls, *i.e.* that, here, adhesion to the plates is weaker than gel cohesion. We have been able to check that relation (1) holds, not only for the $\sigma \geq 10\,$Pa data of fig. 2, but, as well, with the 4 wt% samples of fig. 4, for $\sigma \geq 7\,$Pa.

The distinction between stages II and III in the above scenario remains, at this stage, quite speculative. In order to gain further insight into the nature of the microstructures, we performed, on 4 wt% gels at $T = 23\,^\circ$C, the following set of experiments. We let gelation proceed under $\sigma = 15\,$Pa up to a predefined η_σ level. The corresponding $\eta_\sigma(t)$ curve is displayed in fig. 5a. When this state is reached, at time t_w after the end of the quench, we ramp the stress down to zero within 2 seconds, then commute to a strain ramp at rate $1\,{\rm s}^{-1}$, and measure the stress response. We separately measure, at the same $\dot{\gamma}$ value, the response $\sigma^{(0)}(\gamma)$ of a quiescent gel *of the same age* t_w.

The evolution of $\sigma^{(0)}(\gamma)$ with t_w is shown in fig. 5b. As analyzed by Bot *et al.* [15], it presents an initial elastic, strain hardening part. This elastic regime, ending at a quasi age-independent strain $\gamma_c \sim 350\%$, is followed by a fast drop, after which the system reaches a steady flow regime. We have checked, by raising the cone, that this flow is localized at the upper cell boundary. So, the gel fails by interfacial fracture. As its age t_w increases, the gel becomes gradually stiffer.

Comparison between the sheared and quiescent systems was performed for the states labeled (A) to (D) in fig. 5a, chosen to belong to different stages (I to III) of our scenario and to the fully gelled final state. The results are displayed in figs. 5A to 5D.

Consider first panel D, picturing the response of the sheared system just after full gelation. Up to a strain $\gamma \simeq 200\%$, the initial σ rise, as well as the final steady level, are indistinguishable from those of the isochronous quiescent gel. That is, the age-induced stiffening of the shear modulus of the fully formed gel is basically unaffected by previous shearing. However, the failure stress is considerably smaller than the quiescent one. This is clearly attributable to the relative weakness of the adhesive interface resulting from the recent closure of the last sliding band —which reappears in the post-failure steadily flowing state.

Let us now turn to panel C, pertaining to the earlier stage III. Here again, the initial elastic response is essentially that of the isochronous quiescent gel, but, now, only up to a strain $\simeq 80\%$. However, no well-defined failure threshold can be identified, and the late σ-level lies significantly below the quiescent one. These features appear consistent with our interpretation of stage III in terms of a set of gel layers separated by thin fracture-like sliding bands, bridged by short-lived transient cross-links whose lifetime increases as the stress level is ramped down. Upon reloading, their age is much smaller than that of the already gelled, stiffer, layers. The fact that the small strain modulus is practically equal to the quiescent one thus proves that, in state C, the flow was localized on an overall thickness much smaller than the gap size. Finally, the lower late σ-level is consistent with the presence of several non-interfacial bands.

In contradistinction with the C response, in state B, belonging to stage II, the slope of the initial stress rise is distinctly smaller than its quiescent counterpart. Elasticity in the unloaded state is no longer completely controlled by that of the stiffer regions. This indicates that, in stage II, a sizable fraction of the system is liquid-like, a statement supported by the fact that the late σ-level is significantly smaller than in C.

These features are even more marked in state A, which corresponds to a quasi-crowded microgel suspension. The initial rise is sublinear, but extends over a time ($\sim 2\,$s) much too large to correspond to a viscous transient of the initial (A) suspension. This low-frequency viscoelastic behavior has been characterized by de Carvalho and Djabourov [6] who found that, after unloading from a state close to crowding, at $\nu = 1\,$Hz, $G'/G'' \sim 2$: most probably, during unloading, full percolation has already taken place, leading to a weak gel which behaves as a yield stress fluid [16].

The information emerging from this set of unloading-reloading experiments, though indirect, is consistent with our qualitative scenario. We will now look for further confirmation by investigating the dynamical evolution under various levels of imposed external shear rates.

4 Gelation at imposed strain rate

We perform these experiments at a set of strain rate values $\dot{\gamma}_i$ ($i = 1, \ldots, 6$), chosen to span the various regimes defined above. They are indicated in fig. 6, which displays the same data as fig. 2, now plotted as $\dot{\gamma}_\sigma(t)$. The dashed curves in fig. 6 indicate the loci of the viscosity values characteristic of transitions between the stages defined above.

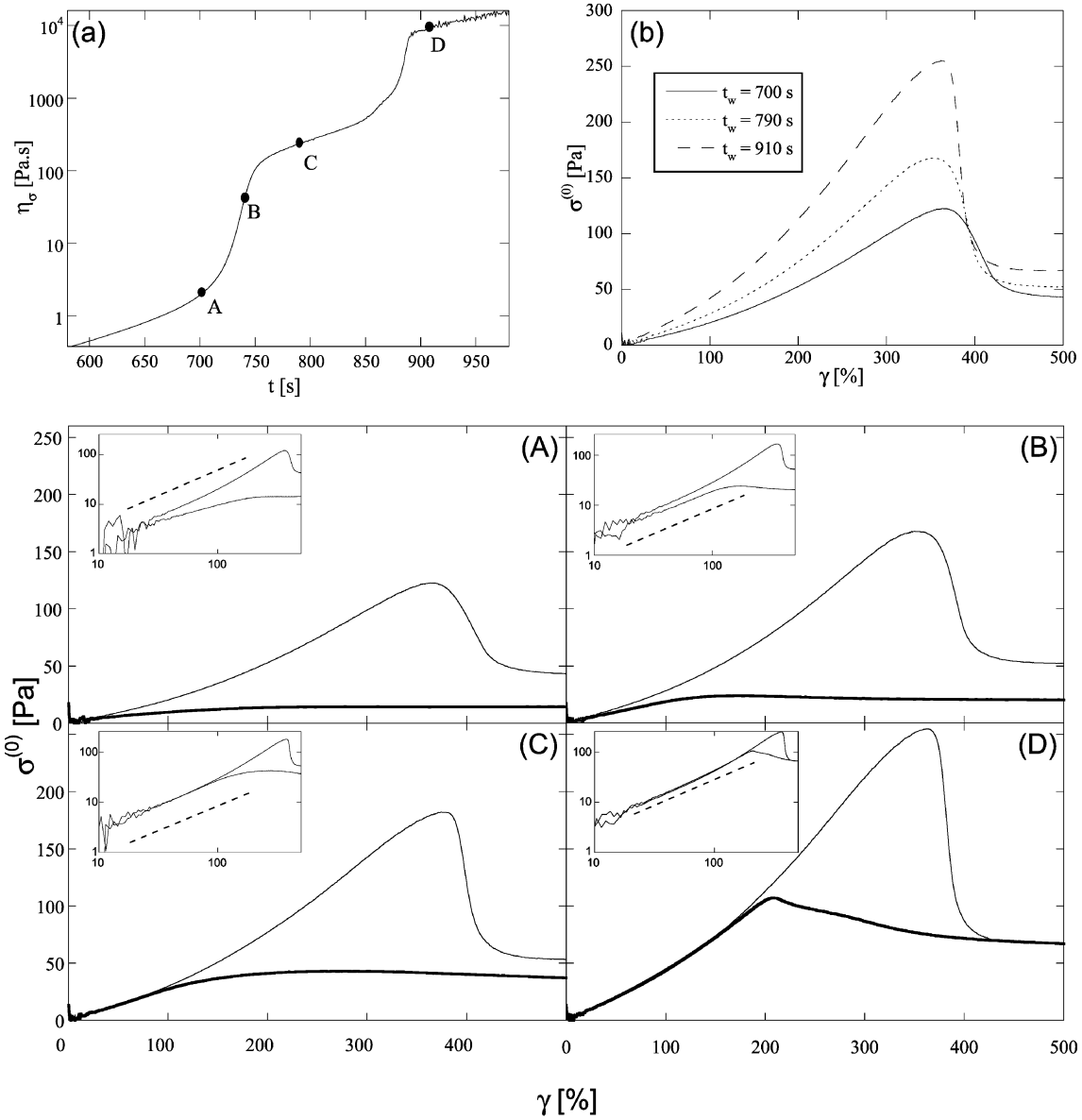

Fig. 5. (a) Viscosity *vs.* time for gelation under stress $\sigma = 15\,\mathrm{Pa}$. (b) Stress $\sigma^{(0)}$ *versus* strain γ start-up responses of gels formed under quiescent conditions. Loading at strain rate $1\,\mathrm{s}^{-1}$ is started at gels ages $t_w = 700, 740, 910\,\mathrm{s}$ after quench, chosen to correspond to points A, B and D on panel (a). Panels (A) to (D): stress responses after unloading at A to D (panel (a)) and immediate reloading (see text). Thin lines: responses of the corresponding isochronous quiescent gels. Inserts: log-log plots of same data, the dashed lines have slope 1. All data are for 4 wt% gelatin in water solutions at $T = 23\,^\circ\mathrm{C}$.

They exhibit a marked curvature. That is, contrary to the claim made in [6], interstage transitions, in particular the crowding one, corresponding to $\eta = \eta_1$ do not correspond to constant shear rate thresholds.

Figure 7 shows the stress responses $\sigma_{\dot\gamma}(t)$ (panel (a)) and the associated apparent viscosities $\eta_{\dot\gamma}(t)$ (panel (b)). Note that, while the stress curves for increasing $\dot\gamma$ do not exhibit any systematic trend, viscosities are clearly ordered: at a given time, the higher $\dot\gamma$, the lower $\eta_{\dot\gamma}$. We now concentrate on the structure of these curves.

In regime I (curve 1), after an initial fast rise, the smooth growth of $\eta_{\dot\gamma}$ slows down without showing any trend toward saturation, and we find that higher shear rates (data not shown) result in lower viscosity levels. This agrees with the conclusions of ref. [6] that, in this fast-shearing regime, the flowing system consists of a non-crowded suspension of microgel particles whose size is a decreasing function of $\dot\gamma$. The late thickening indicates that this structure is not truly stationary, but exhibits very slow coarsening via either chain accretion or inter-particle aggregation.

As $\dot\gamma$ is decreased to $\dot\gamma_2 = 0.5\,\mathrm{s}^{-1}$, the previous smooth response exhibits a spectacular change: a considerable ruggedness develops on top of the overall viscosity increase. This low-frequency, broad-band noise is precisely what can be expected from the structure we have proposed

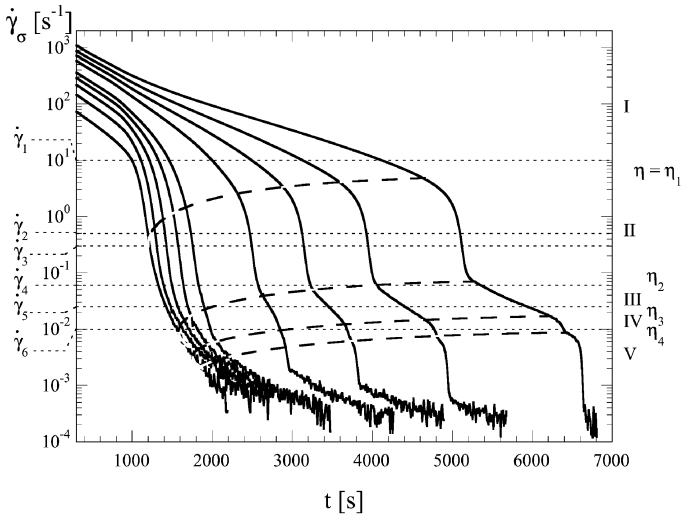

Fig. 6. Same data as in fig. 2, plotted as strain rate $\dot\gamma_\sigma$ *vs.* time t. σ increases from left to right. The dashed lines indicate the limits ($\eta = \eta_i$) between the various regimes (I to IV); they have been built by interpolating between points obtained for each σ, by determining from fig. 2 the value of $\dot\gamma_\sigma$, where $\eta_\sigma = \eta_i$ (from top to bottom $i = 1, \ldots, 4$). Dotted lines: $\dot\gamma$-levels corresponding to the data shown in fig. 7.

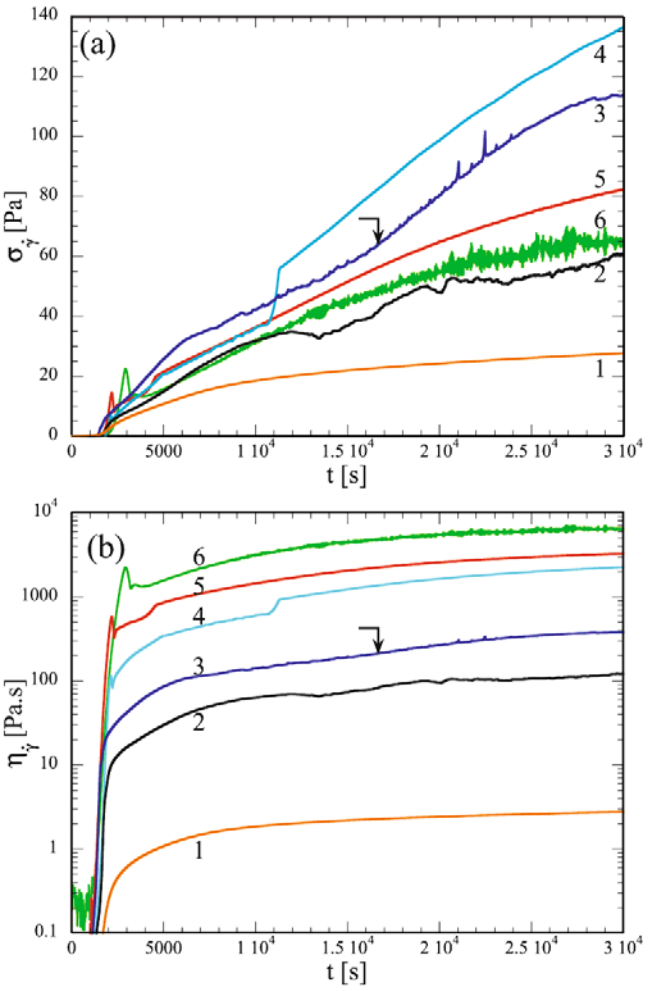

Fig. 7. (a) Stress $\sigma_{\dot\gamma}$ *versus* time during gelation at imposed strain rate of a 5 wt% sample. Curves 1 to 6 correspond to $\dot\gamma$ values of 10; 0.5; 0.3; 0.06; 0.025; 0.01 s^{-1}. The arrow indicates the time at which the sample gelling under $\dot\gamma_3 = 0.3\,\mathrm{s}^{-1}$ crosses the boundary between regime II and III. (b) Same data as in (a), plotted as apparent viscosity $\eta_{\dot\gamma}$ *versus* time.

for stage II, made of coalescing strata intermittently bridging and breaking under shear. Note (fig. 7) that, for $\dot\gamma = \dot\gamma_2$, η remains smaller than the value $\eta_2 = 220\,\mathrm{Pa\,s}$ which signals the end of stage II over the full experimental time window ($t < 3 \cdot 10^4\,\mathrm{s}$). This contrasts with the data obtained at $\dot\gamma_3 = 0.3\,\mathrm{s}^{-1}$, for which η becomes larger than η_2 for $t \geq 16600\,\mathrm{s}$ (see arrow in fig. 7). As can be seen most easily on panel (a), as long as the system is in regime II, the same type of ruggedness as in the previous case is observed. However, as dynamic thickening brings it gradually deeper into stage III, the amplitude of the broad-band fluctuations decreases while spike-noise becomes increasingly prevalent. These spikes we believe to be the signature of the localized, transient, closure/fracture events between the thickening strata evoked in the previous section.

Curves 4 and 5, which correspond to smaller $\dot\gamma$ values, present two strong new qualitative features: i) a viscosity overshoot, the amplitude of which increases as $\dot\gamma$ decreases, develops at the end of the initial fast rise; ii) the subsequent slower thickening is interrupted by a clearly marked step. The latter is absent for our smallest strain rate value $\dot\gamma_6 = 0.01\,\mathrm{s}^{-1}$.

Let us first concentrate on curve 6. We note that the viscosity level just after the overshoot $\eta \simeq 1500\,\mathrm{Pa\,s}$ lies in the vicinity of the characteristic value η_4 which marks the closure of one of the two terminal interfacial sliding bands. We thus conclude that the system reaches a fully percolated, though weak, gel state, then fails —hence the overshoot— via a single interfacial fracture. Once this state is reached, as the gel ages it stiffens, *i.e.* its mesh size ξ decreases, and so does the thickness of the sliding band, resulting in the gradual increase of the apparent viscosity.

We propose that, at the slightly larger shear rates $\dot\gamma_4$, $\dot\gamma_5$, after the failure signaled by the overshoot, the system reaches a state corresponding to stage III, and that the η step marks the transition from two to one sliding interfacial bands. However, now, this closure occurs at imposed apparent strain rate, and the amplitude of the η jump depends on the functional form of the band rheology $\sigma = f(\dot\gamma_{\mathrm{loc}})$. In a previous study [17] we have shown that, for a gelatin gel sliding upon glass, the frictional stress σ results from viscous dissipation in an interfacial shear band, with

$$\sigma \sim \dot\gamma_{\mathrm{loc}}^{\alpha}, \qquad \alpha \simeq 0.4. \tag{2}$$

Let us assume that such a power law rheology also holds in the present case, and that the two bands have equal thicknesses. Then, since closing one among the two bands results in a twofold increase of $\dot\gamma_{\mathrm{loc}}$ in the remaining last one, one immediately finds that the ratio of apparent viscosities

across the step should read

$$\eta^{1\text{band}}/\eta^{2\text{bands}} = 2^{\alpha}. \quad (3)$$

The data of curve 4 (respectively, 5) yield for this ratio a value of 1.48 (respectively, 1.42), that is, from eq. (3), an exponent $\alpha \approx 0.5$, in reasonable agreement with the above-mentioned value, a result nicely consistent with our sequential interfacial band closure scenario.

5 Conclusion

The set of experiments presented here confirms the qualitative result of [6], namely: when gelling under fast enough shear rates, gelatin does not reach a fully percolating network state but, rather, forms a slowly aging microgel suspension.

However, we do not confirm the existence of their proposed critical *strain rate* value $\dot{\gamma}^{\star}$. Rather, our results lead us to conclude that the end of the microgel suspension regime corresponds to a critical *viscosity* η_1 hence the departure from horizontality of the dashed curves of fig. 6, which mark the inter-regime boundaries. Of course, the larger $\dot{\gamma}$, the more extended in time the suspension regime will be. This extension might even diverge at some finite large strain rate threshold, beyond which a microgel suspension would be fully stabilized.

One step beyond, we have shown here that under lower shearing rates, gels form via a complex dynamical process resulting from competition between the trend to chain aggregation and the disrupting effect of shear. That this latter effect is important in the case of gelatin is clearly due to the relative weakness of the H-bonds involved in the formation of the triple helix cross-link segments. More generally, it should also come into play in gelation under shear for all materials forming reversible gels.

Moreover, the analysis of the detailed evolution of the rheological responses of such a physically cross-linked system enables us to conclude to anisotropic, stratified gelation, associated with increasing flow localization. However the aging dynamics characteristic of gelatin necessarily leads to a rather fast evolution of such structures upon cessation of shear. So, in order to test the shear-induced anisotropic structuration suggested by our analysis, it will be necessary to try and stabilize these structures, which should give rise to toughness anisotropy, by using gel-forming materials presenting much slower aging —such as, possibly, agar [1,18].

We are grateful to A.N. Morozov for fruitful discussions on this and related subjects.

References

1. N. Altmann, J.J. Cooper-White, D.E. Dunstan, J.R. Stokes, J. Non-Newtonian Fluid Mech. **124**, 129 (2004).
2. I.T. Norton, D.A. Jarvis, T.J. Foster, Int. J. Biol. Macromol. **26**, 255 (1999).
3. A. Gabriele, F. Spyropoulos, I.T. Norton, Food Hydrocolloids **23**, 2054 (2009).
4. A. Omari, G. Chauveteau, R. Tabary, Colloids Surf. A **225**, 37 (2003).
5. M. Caggioni, P.T. Spicer, D.L. Blair, S.E. Lindberg, D.A. Weitz, J. Rheol. **51**, 851 (2007).
6. W. de Carvalho, M. Djabourov, Rheol. Acta **36**, 591 (1997).
7. K. te Nijenhuis, *Thermoreversible Networks*, Adv. Polym. Sci. **130**, 1 (1997).
8. S. Manneville, Rheol. Acta **47**, 301 (2008) and references therein.
9. C. Baravian, D. Quemada, Eur. Phys. J. AP **2**, 189 (1998).
10. O. Ronsin, C. Caroli, T. Baumberger, Phys. Rev. Lett. **103**, 138302 (2009).
11. P.M. Gilsenan, S.B. Ross-Murphy, Int. J. Biol. Macromol. **29**, 53 (2001).
12. L. Guo, R.H. Colby, C.P. Lusignan, T.H. Whitesides, Macromolecules **36**, 9999 (2003).
13. J. Sprakel, E. Spruijt, M.A. Cohen Stuart, M.A.J. Michels, J. van der Gucht, Phys. Rev. E **79**, 056306 (2009).
14. J.-F. Berret, Y. Séréro, Phys. Rev. Lett. **87**, 048303 (2001).
15. A. Bot, I.A. van Amerongen, R.D. Groot, N.L. Hoekstra, W.G.M. Agterof, Polym. Gels Networks **4**, 189 (1996).
16. G.M. Kavanagh, S.B. Ross-Murphy, Prog. Polym. Sci. **23**, 533 (1998).
17. T. Baumberger, C. Caroli, O. Ronsin, Eur. Phys. J. E **11**, 85 (2003).
18. V. Normand, D.L. Lootens, E. Amici, K.P. Plucknett, P. Aymard, Biomacromolecules **1**, 730 (2000).